Supplementary Material

Surface functionalization of the endotracheal tubes coated by laccase-gadolinium phosphate hybrid nanoparticles for antibiofilm activity and contrasting properties

Anita Azmi[a,b,#], Somayeh Mojtabavi[a,#], Seyed Ali Asghar Fakhrmousavi[c], Mehrdad Faizi[b], Hamid Forootanfar[d], Nasrin Samadi[a], and Mohammad Ali Faramarzi[a,*]

[a] *Department of Pharmaceutical Biotechnology, Faculty of Pharmacy, Tehran University of Medical Sciences, P.O. Box 14155−6451, Tehran 1417614411, Iran*

[b] *Department of Pharmacology & Toxicology, Faculty of Pharmacy, Shahid Beheshti University of Medical Sciences, Tehran, Iran*

[c] *Department of Internal Medicine, Guilan University of Medical Sciences, Rasht, Iran*

[d] *Department of Pharmaceutical Biotechnology, Faculty of Pharmacy, Kerman University of Medical Sciences, Kerman, Iran*

---

[*]Corresponding author: M.A. Faramarzi, Telefax: +98-21-66954712, E-mail: faramarz@tums.ac.ir

[#]A. Azmi and S. Mojtabavi contributed equally as the first author.

S1. Preparation of laccase@$GdPO_4$•HNPs

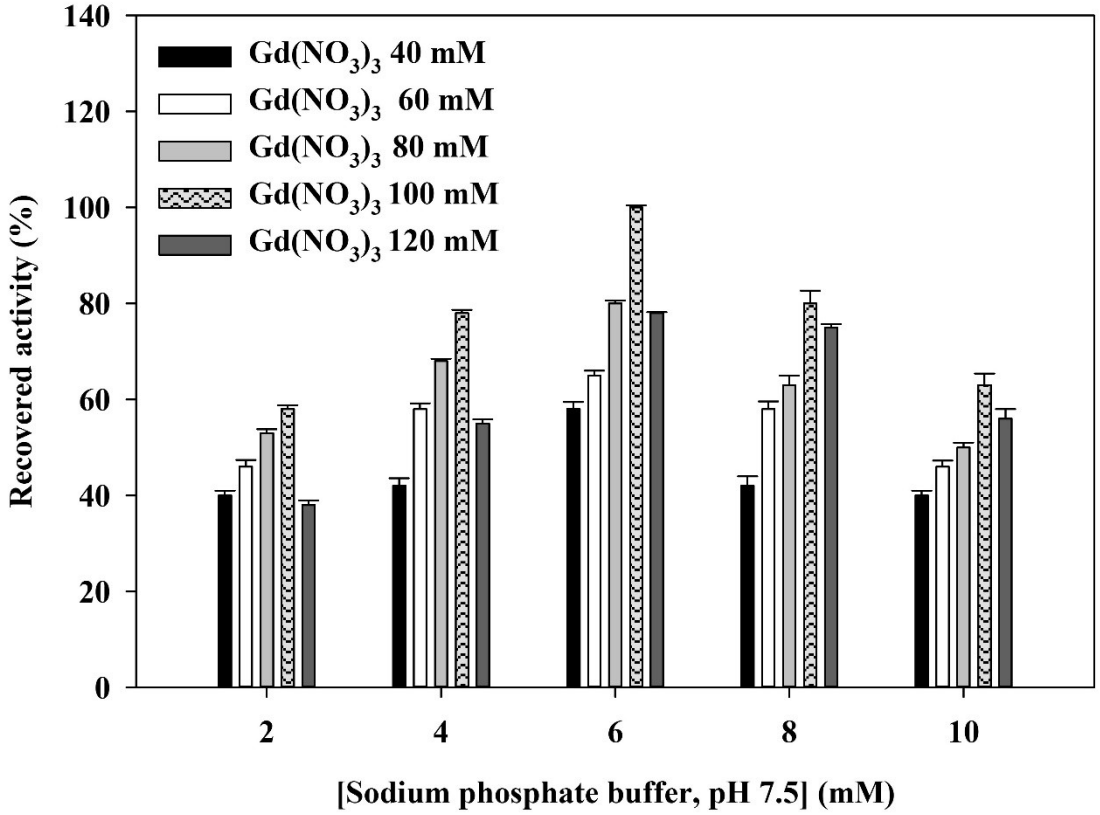

Figure S1. The effect of phosphate buffer (2–10 mM, pH 7.5) and gadolinium nitrate (40–120 mM) on the activity of laccase@$GdPO_4$•HNPs. The experiments were independently repeated three times and the error bars represent the standard deviation of a data set (n=3).

S2. Characterization of the fabricated HNFs

Instrumental analyses were applied to obtain structural information on the constructed enzyme-inorganic HNPs. SEM was used to verify the morphological differences between nanostructures in the non-immobilized and immobilized states of laccase. SEM images of $GdPO_4$•NPs showed sand-like spherical particles with uniform size and smooth surfaces (Fig. S2). However, no morphological change was evident after the preparation of laccase@$GdPO_4$•HNPs. Furthermore, the elemental constitution of the synthesized NPs and HNPs was subjected to EDX investigation (Fig. S3). The EDX patterns proved the presence of some elements in both samples, which were oxygen (O), phosphorus (P), and gadolinium (Gd). However, laccase@$GdPO_4$•HNPs exhibited a higher mass fraction of copper (Cu), nitrogen (N), and sulfur (S) content undoubtedly validating the laccase association in the HNPs. The structures of $GdPO_4$•NPs and laccase@$GdPO_4$•HNPs were also characterized by FTIR spectra (Fig. S4). For both samples, the adsorptions at 725–1400 cm^{-1} could be assigned to the asymmetric stretching vibration of $(PO_4)^{3-}$ [1]. The chemical interactions between Gd^{3+} and $(PO_4)^{3-}$ were identified by intense transmission bands at 3410–3417 cm^{-1} [2, 3]. The broad adsorption at 3200–3600 cm^{-1} was attributed to the stretching vibration of the O–H and –NH groups [1]. To further prove the inorganic composition of HNPs, XRD analysis was performed (Fig. S5). The obtained peaks' positions of laccase@$GdPO_4$•HNPs were matched with the standard gadolinium phosphate ($GdPO_4$) pattern (JCPDS 00-032-0386) [3]. Hydrodynamic diameters and zeta potentials of NPs in the presence and absence of laccase are reported in Fig. S6. The mean and cumulative size distribution for the prepared HNPs was about 75 and 130 nm, respectively. Also, the zeta potential value (−42.6 mV) for laccase@GdPO4•HNPs showed excellent colloidal stability leading to minimizing particle aggregation. The immobilization of laccase into the HNPs was further studied by TGA (Fig. S7). For $GdPO_4$•NPs, one weight loss stage (48.4%) was clearly distinguished due to dehydration at 80 ºC to 120 ºC. The curve of

laccase@GdPO4•HNPs showed two separable steps of thermal weight loss *i.e.*, the initial dehydration at 80 ºC to 150 ºC and the decomposition of laccase (37.1%) in the temperature range of 250 ºC to 400 ºC.

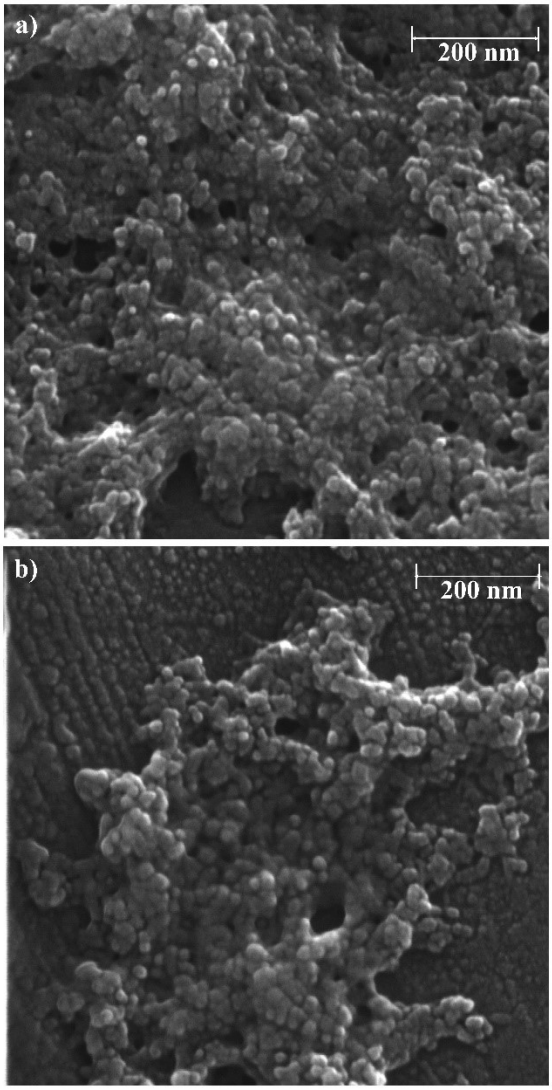

Figure S2. Scanning electron microscope (SEM) imaging of (a) $GdPO_4$•NPs and (b) laccase@$GdPO_4$•HNPs. The immobilization was performed in phosphate buffer (6 mM, pH 7.5) containing laccase activity of 0.1 U mL^{-1} at 25 °C.

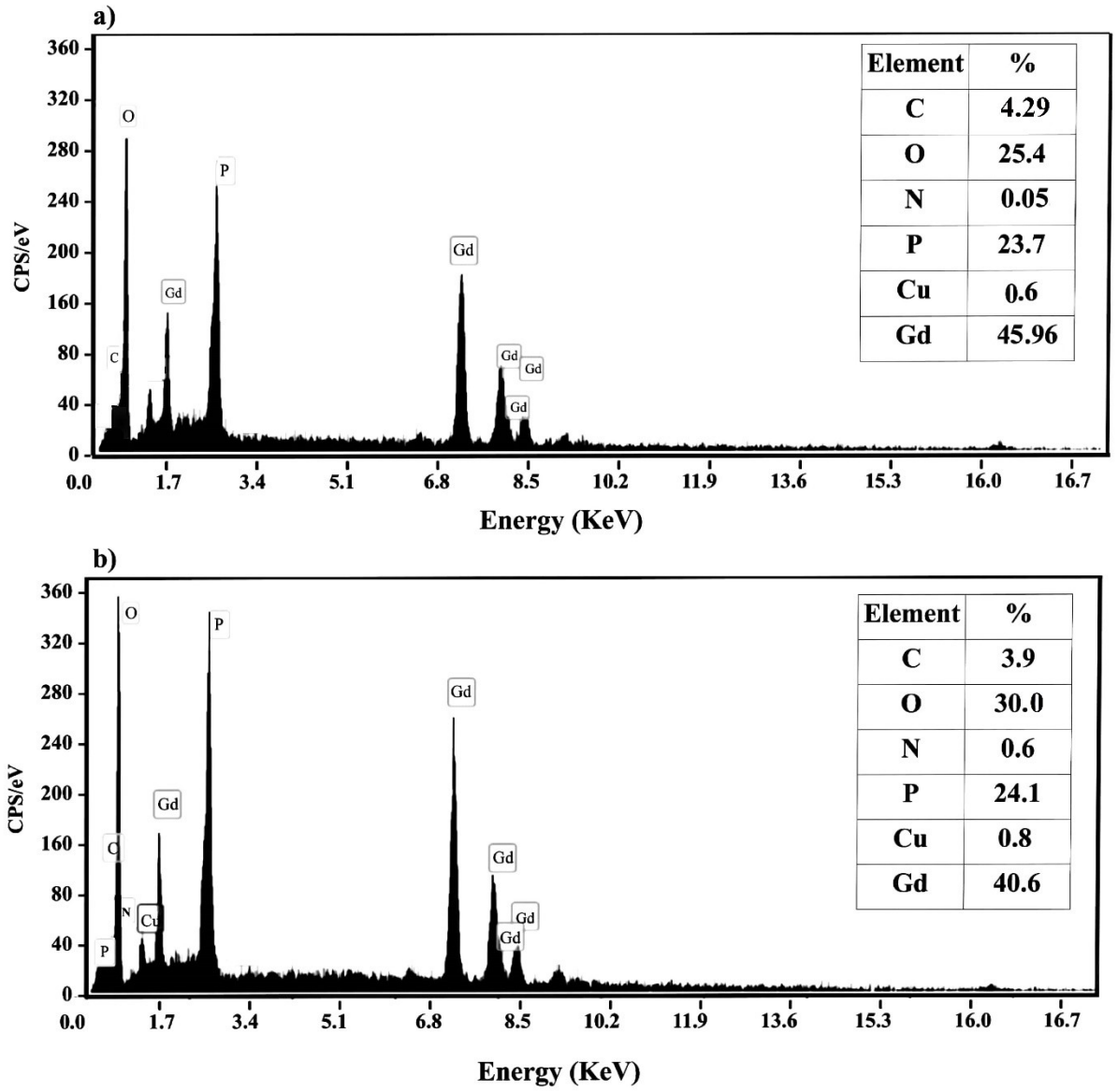

Figure S3. Energy dispersive X-ray analysis (EDX) analysis of (a) $GdPO_4$•NPs and (b) laccase@$GdPO_4$•HNPs prepared in phosphate buffer (6 mM, pH 7.5) using laccase (0.1 U mL^{-1}) and $GdNO_3$ (100 mM).

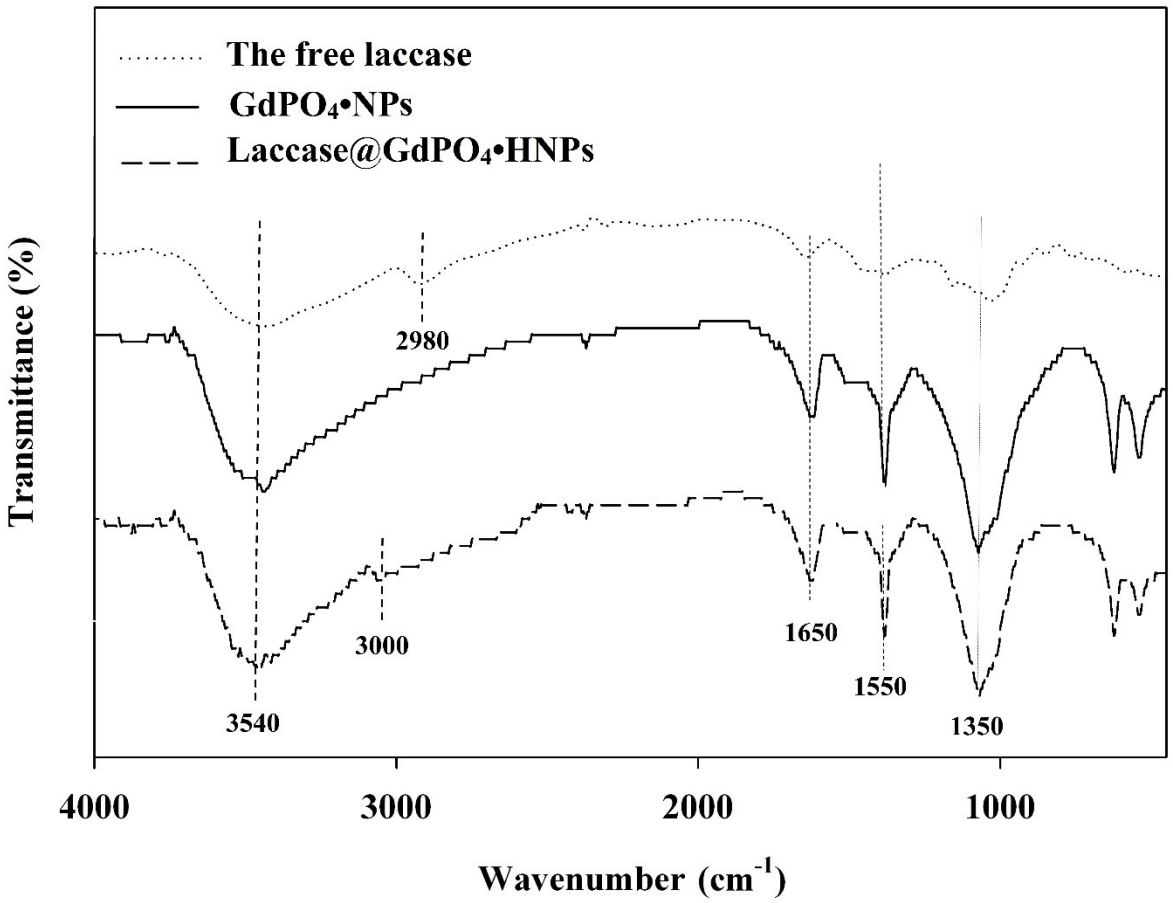

Figure S4. Comparison of the flourier transform infrared (FTIR) of the free enzyme, $GdPO_4$•NPs, and laccase@$GdPO_4$•HNPs from 4000 to 400 cm^{-1}.

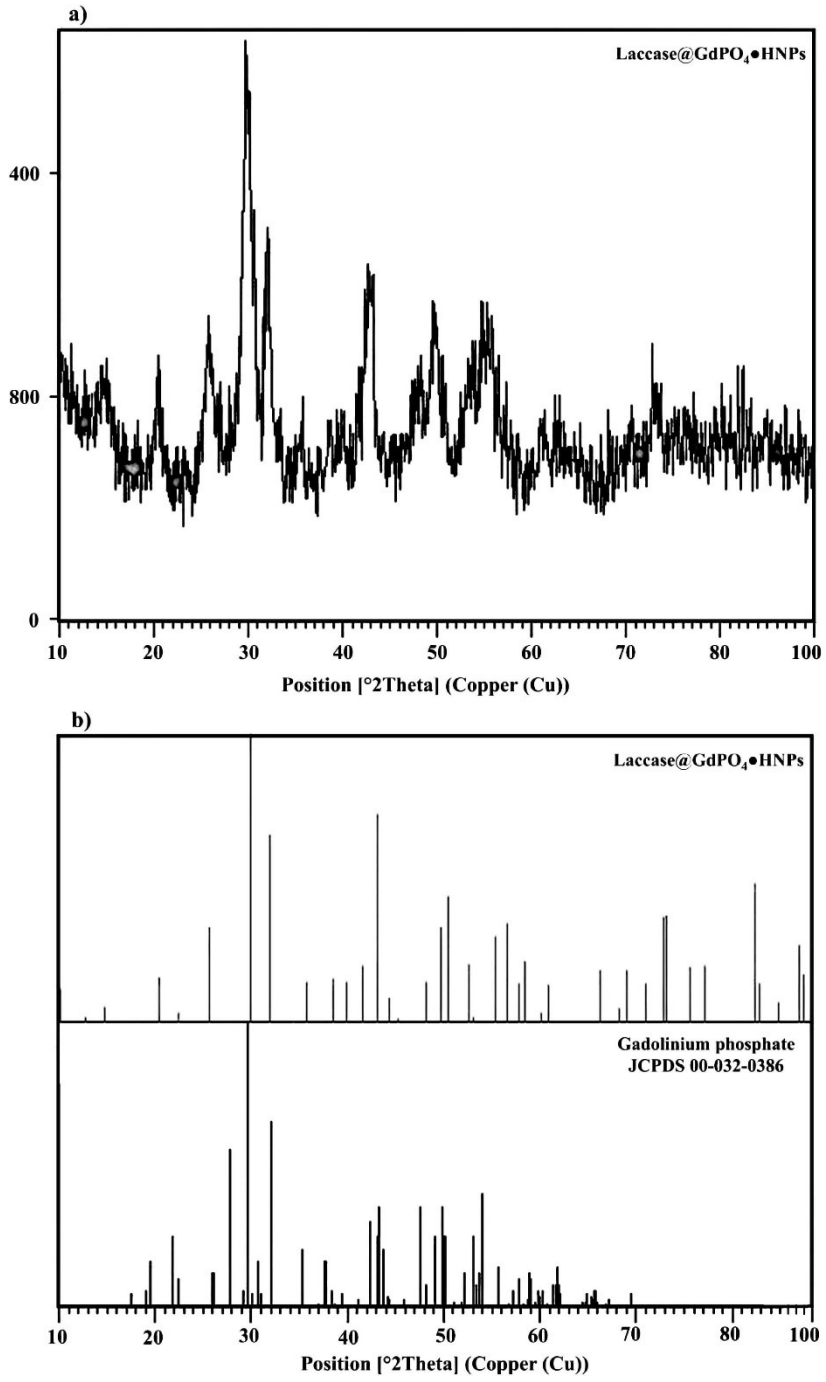

Figure S5. (a) X-ray diffraction analysis (XRD) diffraction pattern of laccase@$GdPO_4$•HNPs and (b) peak list of laccase@$GdPO_4$•HNPs and standard $GdPO_4$•NPs.

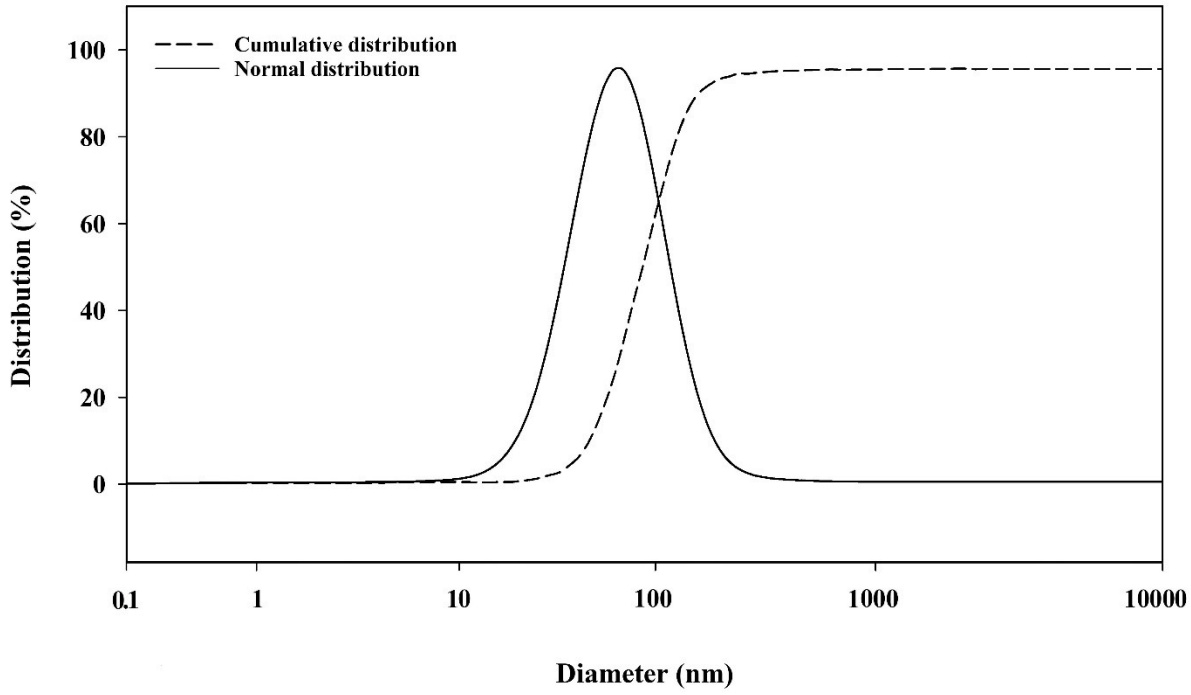

Figure S6. Particle size distribution of laccase@$GdPO_4$•HNPs using dynamic light scattering (DLS) analysis at 25 °C.

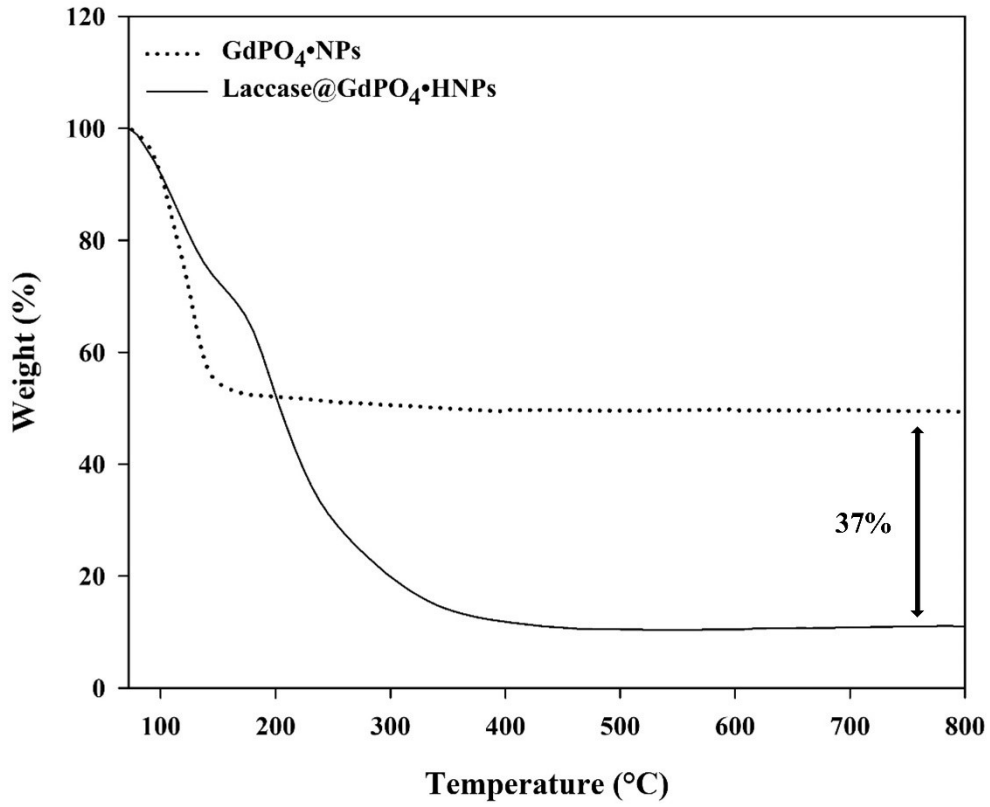

Figure S7. Thermogravimetric analysis (TGA) of (a) $GdPO_4$•NPs and (b) laccase@ $GdPO_4$•HNPs. The temperature increased at a rate of 10 °C min^{-1} from 50 to 800 °C.

S3. Determination of kinetic parameters

Kinetic parameters of the free and immobilized laccase were calculated for ABTS as a water-soluble reducing substrate. The enzymatic oxidation of the substrate at the concentration range of 12 to 360 μM in citrate buffer (100 mM, pH 4.5) was monitored spectrophotometrically at 420 nm. Michael's constant (K_m) and maximum velocity (V_{max}) were evaluated by a Lineweaver-Burke curve. Sequentially, turnover number (K_{cat}) and catalytic efficiency were also obtained by Eq. S1 and Eq. S2, respectively; where [E] is the concentration of the enzyme.

$$K_{cat} = V_{max} / [E] \qquad \text{Eq. S1}$$

$$\text{Catalytic efficiency} = K_{cat} / K_m \qquad \text{Eq. S2}$$

Compared to the free enzyme, the K_m value of laccase did not significantly change after immobilization, however, the V_{max} value for the biocatalyst slightly increased from 7.2 to 7.8 μmol min^{-1} (Table S1). Consequently, substrate accessibility was very similar to that of the free enzyme. The enhanced V_{max} may be related to the high surface area of the prepared HNPs or a cooperative effect of the encapsulated laccase to overcome mass-transfer limitations or favorable conformation of the enzyme after immobilization [4]. Here, the k_{cat} value of the HNPs was higher than the free laccase, confirming their stronger ability for catalysis. According to previous studies, the V_{max} values of laccase entrapped in $Co_3(PO_4)_2$ and $Cu_3(PO_4)_2$ hybrid nanoflowers (HNFs) were 1.8 and 2 folds, respectively, lower than that of the corresponding free enzyme [5, 6]. Furthermore, at the same conditions, laccase@$Co_3(PO_4)_2$•HNFs showed a V_{max} of 4.7 μmol min^{-1} compared with the value of 7.8 μmol min^{-1} for the prepared laccase@$GdPO_4$•HNPs. In any comparison, it must be noted that better catalytic property indicates less enzyme usage in industrial reactions, resulting in lower costs [7].

Table S1. The immobilization yield (%) and efficiency (%) for laccase encapsulated in $GdPO_4$ hybrid nanoparticles (HNPs) and kinetic parameters of the prepared

laccase@$GdPO_4$•HNPs (0.1 U mL^{-1}) for oxidation of ABTS (12–360 μM, 12 μM intervals) compared to the free enzyme (Mean ± SD, n = 3).

Parameter	**The free laccase**	**Laccase@$GdPO_4$•HNPs**
V_{max} (μmol min^{-1})	7.2 ± 0.2	7.8 ± 0.3
$K_m \times 10^8$ (μM)	2.1 ± 0.1	2.0 ± 0.1
$K_{cat} \times 10^{-2}$ (s^{-1})	8.6 ± 0.4	9.3 ± 0.6
Catalytic efficiency $\times 10^{-10}$ (K_{cat}/K_m)	4.0 ± 0.2	4.7 ± 0.4
Immobilization yield (%)	83.0 ± 0.5	
Immobilization efficiency (%)	82.1 ± 0.6	

S4. Evaluation of the activity and stability of laccase@$GdPO_4$•HNPs

The activity of laccase@$GdPO_4$•HNPs was measured in a temperature range of 25–55 °C (10 °C intervals) and pH 2.5–8.5 (pH 1 intervals). For the purpose of stability study, the synthesized biocatalyst was incubated for 3 h at the above-mentioned pH and temperature ranges. The following buffers were incorporated into the experiments including glycine-HCl buffer (100 mM, pH 2.5), citrate buffer (100 mM, pH 3.5–6.5), and phosphate buffer (10 mM, 7.5–8.5). Subsequently, the residual activity of the samples was measured. Values obtained from the activity and stability of the fabricated biocatalyst were compared with the free enzyme as the positive control. All assays were average of three repetitions, and the results were expressed as the mean ± standard deviation (SD). As depicted in Fig. S8, the proper pH (4.5) and temperature (40 °C) were nearly the same for the specific activity of the free and encapsulated enzyme. Compared to free laccase, the immobilized enzyme exhibited significantly improved activity between pH ranges of 2.5–6.5 and temperatures of 20–50 °C, while it remained particularly unchanged as pH increased above 6.5. Under the temperature of 40 °C and pH 4.5, the HNPs were more efficient than laccase@$Co_3(PO_4)_2$•HNFs with an average specific activity of 6.2 and 5 U mg^{-1}, respectively. This improvement could be attributed to the high surface area and catalytic activity of HNPs. Such characteristics improved mass transfer and contact with the substrate, thus, increasing the oxidation activity of the enzyme [1, 5].

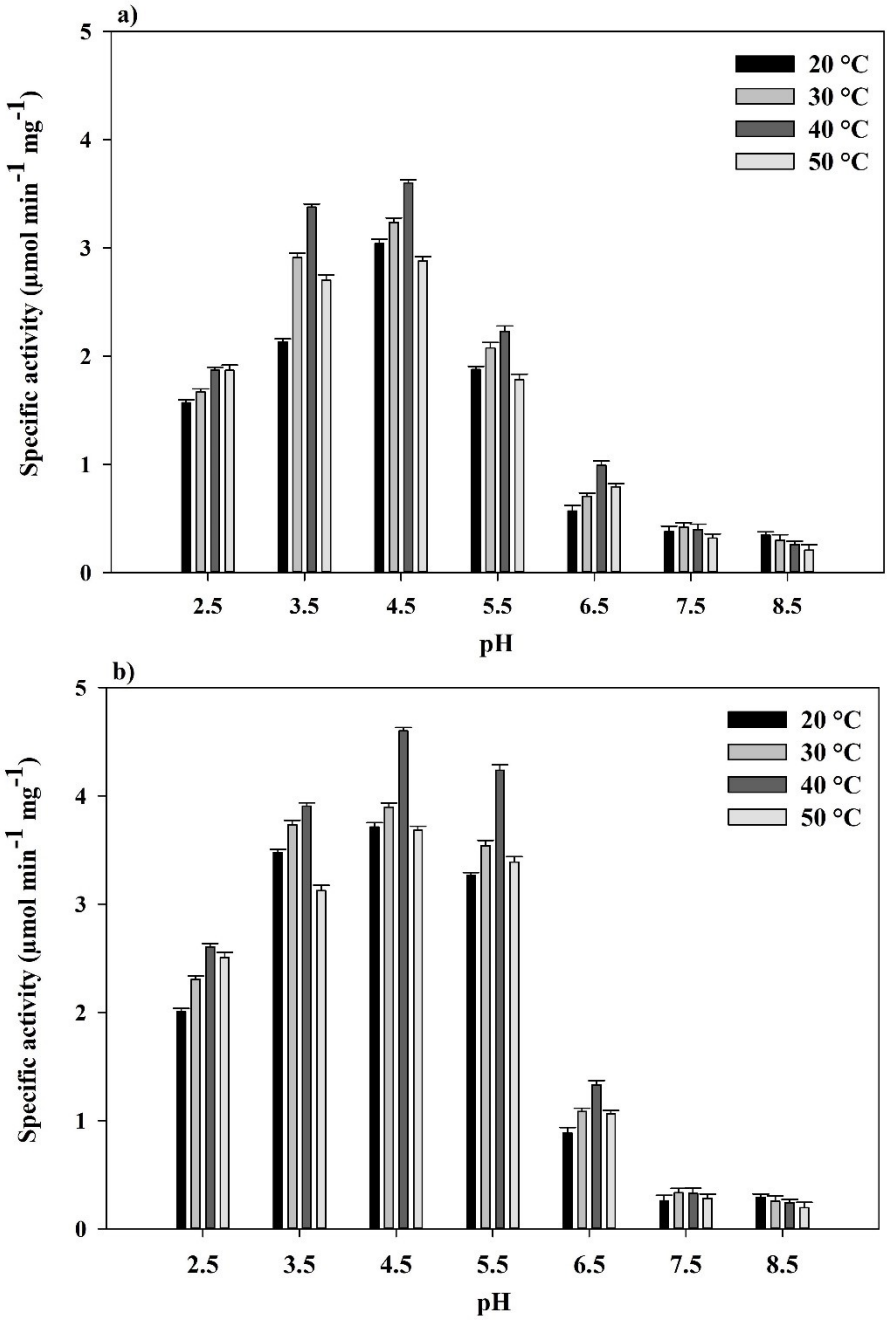

Figure S8. Effect of pH and temperature on the activity of (a) the free enzyme and (b) laccase@$GdPO_4$•HNPs. Error bars show the mean of three independent experiments.

The enzyme stability by immobilization is an important parameter to ensure economic and technical feasibility [5]. In this regard, the stability of the constructed biocatalysts was evaluated after 3 h incubation over a wide range of pH and temperature. As shown in Fig. S9, the constructed HNPs demonstrated greater recovered activity (RA%) than the free laccase at both acidic and alkaline pH conditions, indicating wide pH range tolerance of the hybridized enzyme. For instance, after incubation at pH 3.5 and 8.5, the RA% of immobilized laccase was near 100% and 50%, respectively, while the free enzyme activity dropped to 76% and 5% under the same condition (25 °C). Similarly, the activity of laccase encapsulated in $Cu_3(PO_4)_2$, $Zn_3(PO_4)_2$, and $Co_3(PO_4)_2$•HNSs were retained at about 100%, 85%, and 90% at pH 3.5, respectively [5, 6, 8]. The immobilization of enzymes into HNSs could reduce unfolding, and enhance the stiffness and conformational flexibility of the molecule under severe environmental conditions [9, 10].

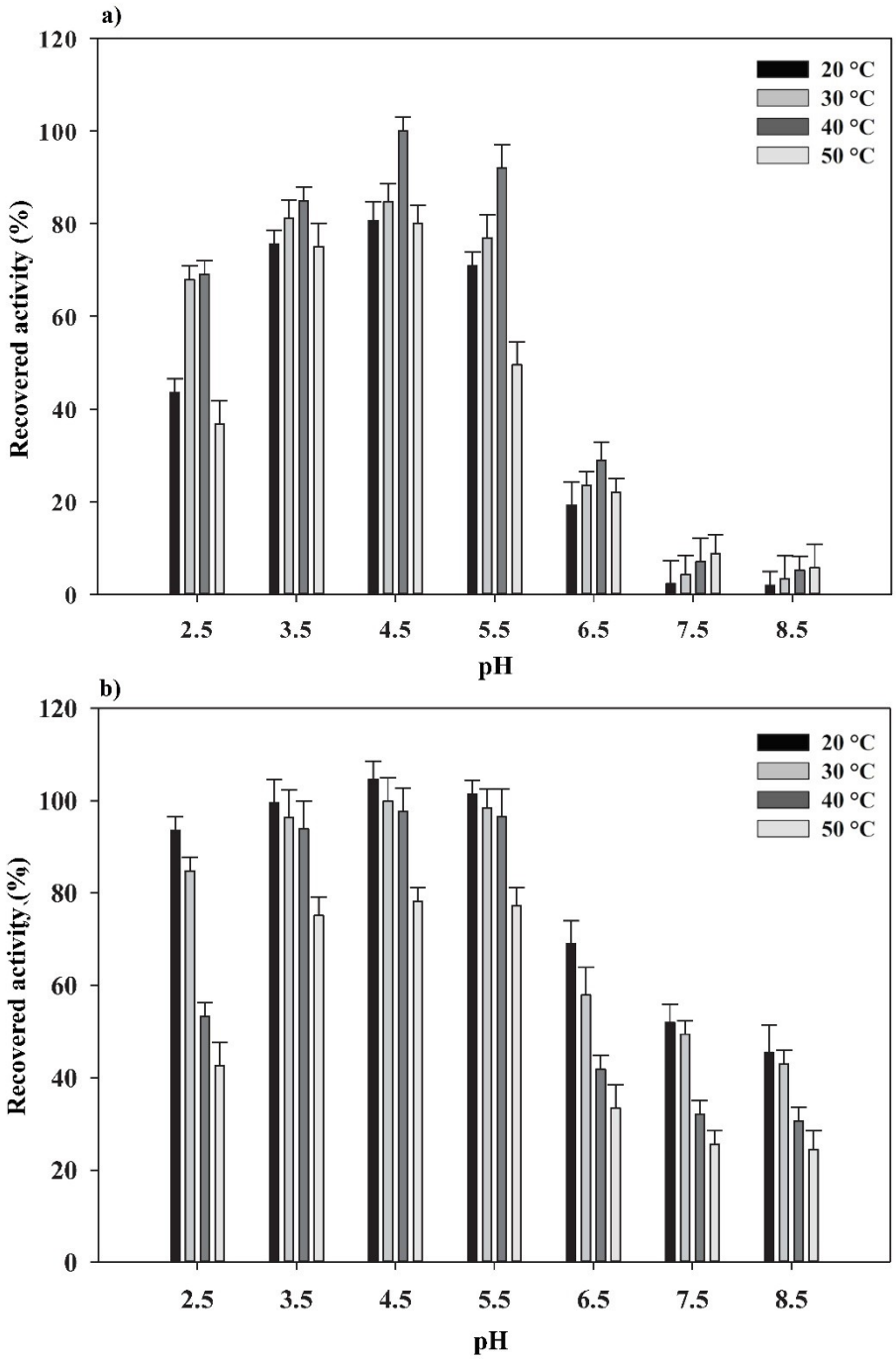

Figure S9. Effect of pH and temperature on the stability of (a) the free enzyme and (b) laccase@$GdPO_4$•HNPs with error bars depicting the standard deviation during three repeated runs of each experiment. The result was established with the highest value of each set being assigned the value of 100% activity.

S5. Reusability and storage stability

The functional and sometimes structural properties of enzymes are often significantly improved after immobilization; thus, they may become more stable and can be used in several subsequent cycles that increase their cost-effectiveness in industrial applications [1]. In order to determine the reusability of the immobilized enzyme, the activity of laccase@$GdPO_4$•HNPs was measured repeatedly. After each assay, the precipitate was collected and washed three times with distilled water. This process was repeated until the catalytic activity dropped to 50% of its initial value. As shown in Fig. S10a, the reusability of the hybridized laccase remained up to 50% of its initial value after 11-cycle reuse. Thus, the fabricated HNPs provided remarkable reusability, which may be due to the structural stability of the immobilized laccase. Nevertheless, the loss of activity during successive cycles might be associated with enzyme denaturation, leaching of the enzyme, or the blockage effect of the enzyme products [9]. Furthermore, the laccase-based nanostructures showed promising reusability; for example, the reusability of laccase immobilized on Fe_3O_4/nylon composite nanoparticles retained less than 40% of their initial activities after 10 runs [10]. Laccase@$Zn_3(PO_4)_2$•HNFs declined 45% of the initial activity after 12 consecutive cycles [1].

The storage stability was evaluated by incubation of the free and immobilized enzyme at 4 and 25 °C, and the residual enzymatic activity was measured for 30 days (5-day intervals). Assay results were averaged over three repetitions, and the results were expressed as mean ± SD. Interestingly, the storage stability of laccase was improved as a result of hybridization. Remarkable differences between the stability of the free and immobilized biocatalysts were observed at each temperature. As illustrated in Fig. S10b, after 20 days of storage at 4 °C, the prepared HNFs retained up to 95% of the initial activity, while the free enzyme lost 30% of its catalytic activity. After 30 days, the free laccase indicated no activity at 25 °C; whereas the immobilized laccase retained 25% of its activity in the same conditions. The results indicate

that the immobilization process has a protective effect on the enzyme's 3D structure, which enhances its storage stability [9].

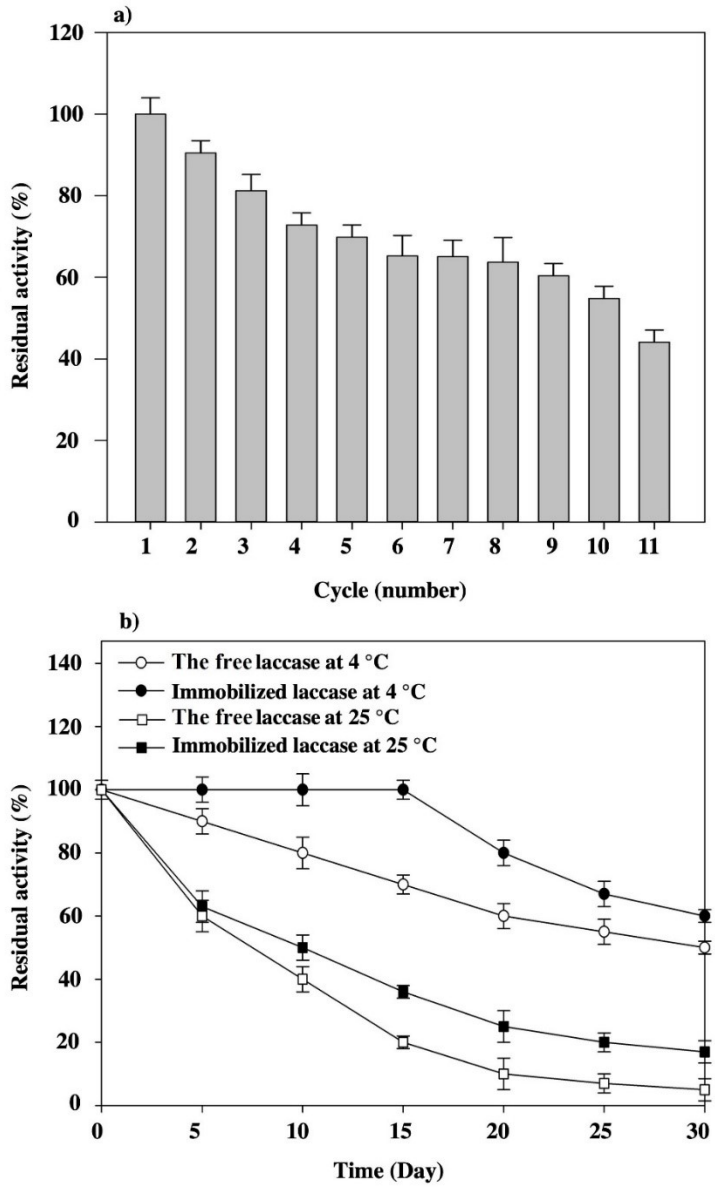

Figure S10. (a) Reusability of laccase@$GdPO_4$•HNPs in citrate buffer (100 mM, pH 4.5) at 40 °C. (d) Storage stability of the free laccase and laccase@$GdPO_4$•HNPs up to 30 days of storage at 4 °C and 25 °C. The results represented in the bar graphs are obtained from three independent experiments.

Additional references

[1] M. Kiani, S. Mojtabavi, H. Jafari-Nodoushan, S.R. Tabib, N. Hassannejad, M.A. Faramarzi, Fast anisotropic growth of the biomineralized zinc phosphate nanocrystals for a facile and instant construction of laccase@$Zn_3(PO_4)_2$ hybrid nanoflowers. Int. J. Biol. Macromol. 204(2022): 520–31. https://doi.org/10.1016/j.ijbiomac.2022.02.023

[2] S.K. Pandey, S. Singh, S.K. Mehta, Biocompatible gadolinium oxide nanoparticles as efficient agent against pathogenic bacteria. J. Colloid Interface Sci. 529(2018): 496–504. https://doi.org/10.1016/j.jcis.2018.06.030

[3] I. Suryawanshi, S. Srinidhi, S. Singh, R. Kalia, R.K. Kunchala, S.L. Mudavath, B.S. Naidu, Downshifting and upconversion dual mode emission from lanthanide doped $GdPO_4$ nanorods for unclonable anti-counterfeiting. Mater. Today Commun. 26(2021): 102144. https://doi.org/10.1016/j.mtcomm.2021.102144

[4] A.H. Memon, R. Ding, Q. Yuan, Y. Wei, H. Liang, Facile synthesis of alcalase-inorganic hybrid nanoflowers used for soy protein isolate hydrolysis to improve its functional properties. Food Chem. 289(2019): 568–74. https://doi.org/10.1016/j.foodchem.2019.03.096

[5] F. Rezayaraghi, H. Jafari-Nodoushan, S. Mojtabavi, S. Golshani, H. Jahandar, M.A. Faramarzi, Hybridization of laccase with dendrimer-grafted silica-coated hercynite-copper phosphate magnetic hybrid nanoflowers and its application in bioremoval of gemifloxacin. Environ. Sci. Pollut. Res. 29(2022): 89255–72. https://doi.org/10.1007/s11356-022-21959-4

[6] K. Vojdanitalab, H. Jafari-Nodoushan, S. Mojtabavi, M. Shokri, H. Jahandar, M.A. Faramarzi, Instantaneous synthesis and full characterization of organic–inorganic laccase-cobalt phosphate hybrid nanoflowers. Sci. Rep. 12(2022): 1–6. https://doi.org/10.1038/s41598-022-13490-w

[7] Y. Ghasemi, Z. Dehdari, M. Mohkam, M. Kargar, Isolation and optimization of cultivation conditions for production of chitinase by *Aeromonas* sp. ZD_05 from the Persian Gulf. J. Pure Appl. Microbiol.7(2013): 913–8.

[8] P. Hariri, H. Jafari-Nodoushan, S. Mojtabavi, N. Hadizadeh, F. Rezayaraghi, M.A. Faramarzi, Magnetic casein aggregates as an innovative support platform for laccase immobilization and bioremoval of crystal violet. Int. J. Biol. Macromol. 202(2022): 150–60. https://doi.org/10.1016/j.ijbiomac.2021.12.099

[9] S.K. Patel, S.V. Otari, Y.C. Kang, J.K. Lee JK, Protein–inorganic hybrid system for efficient his-tagged enzymes immobilization and its application in L-xylulose production. RSC Adv. 7(2017): 3488–94. https://doi.org/10.1039/C6RA24404A

[10] H.Y. Chen, Y. Ting, H.C. Kuo, C.W. Hsieh, H.Y. Hsu, C.N. Wu, K.C. Cheng, Enzymatic degradation of ginkgolic acids by laccase immobilized on core/shell Fe_3O_4/nylon composite nanoparticles using novel coaxial electrospraying process. Int. J. Biol. Macromol. 172(2021): 270–80. https://doi.org/10.1016/j.ijbiomac.2021.01.004